雑誌

発表者氏名	論文タイトル名	発表誌名	巻号	ページ	出版年
K. Suzuki, Shigeto Kobayashi, Kazushige Yamazaki, Masaaki Gondo, Kazuo Tomizawa, Yoshihiro Arimura, Kimimasa Nakabayashi, Shoichi Ozaki, Masaharu Yoshida, Toshiharu Yoshida, Norimasa Tsusaka, Eri Muso, Tomio Okazaki, and Hiroshi Hashimoto.	Analysis of risk epitopes of anti-neutrophil antibody MPO-ANCA in vasculitis in Japan population.	Microbiol.Immunol.	51	1215-1220	2007
Melissa Goedken, Sally McComick, Kevin G. Leidal, Kazuo Suzuki, Yosuke Kameoka, Joshua M. Astern, Meilan Huang, Artem Cherkasov, William M. Nauseef.	Impact of two novel mutations on the structure and function of human myeloperoxidase.	J. Biol. Chem.	282	27994-8003	2007
Akiyoshi Hoshino, Tomokazu Nagao, Toshiko Ito-Ihara, Akiko Ishida-Okawara, Kazuko Uno, Eri Muso, Noriko Nagi-Miura, Naohito Ohno, Kazuhiro Tokunaka, Shiro Naoe, Hiroshi Hashimoto, Masato Yasuhara, Kenji Yamamoto, Kazuo Suzuki.	Trafficking of QD-conjugated MPO-ANCA in Murine Systemic Vasculitis and Glomerulonephritis model mice.	Microbiol Immunol	51	1215-1220	2007
Tomokazu Nagao, Mimiko Matsumura, Ayako Mabuchi, Akiko Ishida-Okawara, Osamu Koshio, Haruyuki Minamitani, and Kazuo Suzuki.	Up-regulation of adhesion molecule expression in glomerular endothelial cells by anti-myeloperoxidase antibody.	Neprol. Dialysis Transplant	22	77–87	2007
鈴木和男	血管炎の病態と好中球	臨床検査	51	1071-1080	2007
Ogawa N, Yano S, Yamane Y, Nishiki M, Yamaguchi T, Tanaka M, Tsukamoto T, Muso E, Sugimoto T	A case of MPO-ANCA positive IgA nephropathy successfully treated with tonsillectomy.	Clin Exp Nephrol	11(4)	326-331	2007
Hashimoto M, Nogaki F, Oida E, Tanaka M, Ito-Ihara T, Nomura K, Liu N, Muso E, Fukatsu A, Kita T, Ono T	Glomerulonephritis induced by methicillin-resistant Staphylococcus aureus infection that progressed during puerperal period.	Clin Exp Nephrol	Mar;11(1)	Jun-92	2007
糟野健司、武曾恵理	1．腎虚血再灌流障害とレドックス発現(腎疾患の病態生理：急性腎不全編)	腎と透析	63(3)	299-303	2007

武曾恵理	血尿(よくある症状35の鑑別診断チャート　３２)	臨床研修プラクティス	4(2)	72-73	2007
武曾恵理、猪原登志子、古宮俊幸	ANCA関連腎炎に伴う血管炎	腎と透析	63(1)	31－34	2007
Ito-Ihara T, Ono T, Nogaki F, Suyama K, Tanaka M, YonemotoS, Fukatsu A, KitaT, Suzuki K, Muso E	Clinical Efficacy of Intravenous Immunoglobulin for Patients with MPO-ANCA-Associated Rapidly Progressive Glomerulonephritis.	Nephron Clin Pract	102(1)	c35-c42	2006
Shimosawa M, Liu N, Uemura K, Muso E, Yoshida H, Ono T	Exacerbating mechanisms mediated by LPS-induced activation of coagulation system in IgA nephropathy model mouse HIGA.	Nephrology	11	A58	2006
宇野賀津子、武曾恵理、尾松芳樹、八木克己、猪原登志子、椛田美由紀、三井氏瑤子、村上善基、谷川真理、稲葉カヨ、鈴木和男、藤田哲也	健常人と各種疾患患者の末梢血のセンダイウイルス刺激IFN-α産生能とプラズマサイトイド樹状細胞数との相関	PASKEN JOURNAL	19	1～6	2006
古宮俊幸、武曾恵理	ＨＩＧＡマウスにおけるＩＬ－１２誘導糸球体装飾での酸化ストレスおよびサイトカインに対するオルメサルタンの影響	Medical Tribune		p17	2006
Veeraveedu PT, Watanabe K, Ma M, Thandavarayan RA, Palaniyandi SS, Yamaguchi K, Suzuki K, Kodama M, Aizawa Y.	Comparative effects of torasemide and furosemide in rats with heart failure.	Biochem Pharmacol.			2008(印刷中)
Okura Y, Ohno Y, Suzuki K, Taneda K, Ramadan MM, Mitsuma W, Tanaka K, Kashimura T, Ito M, Ishizuka O, Kato K, Hanawa H, Honda Y, Kodama M, Aizawa Y.	Characterization of outpatients with systolic dysfunction in a Japanese community by total enumeration. -Sado Heart Failure Study-	Circulation Journal	71	1004-1012	2007
Okura Y,Ohno Y,Ramadan MM,Suzuki K,Taneda K,Obata H,Tanaka K,Kashimura T,Ishizuka O,Kato K,Hanawa H,Honda Y,Kodama M,Aizawa Y.	Characterization of Outpatients With Isolated Diastolic Dysfunction and Evaluation of the Burden in a Japanese Community –Sado Heart Failure Study-.	Circulation Journal	71	1013-1021	2007
Palaniyandi SS, Nagai Y, Watanabe K, Ma M, Veeraveedu PT, Prakash P, Kamal FA, Abe Y, Yamaguchi K, Tachikawa H, Kodama M, Aizawa Y.	Chymase inhibition reduces the progression to heart failure after autoimmune myocarditis in rats.	Exp Biol Med.	232	1213-1221	2007

Veeraveedu PT, Watanabe K, Ma M, Palaniyandi SS, Yamaguchi K, Suzuki K, Kodama M, Aizawa Y.	Torasemide, a long-acting loop diuretic, reduces the progression of myocarditis to dilated cardiomyopathy.	Eur J Pharmacol.			2007(印刷中)
Yanagawa B, Kataoka M, Ohnishi S, Kodama M, Tanaka K, Miyahara Y, Ishibashi-Ueda H, Aizawa Y, Kangawa K, Nagaya N.	Infusion of adrenomedullin improves acute myocarditis via attenuation of myocardial inflammation and edema.	Cardiovasc Res.	76	110-118	2007
佐地　勉	蛋白合成酵素阻害薬ウリナスタチン療法	日本臨床	66(2)	343-348	2008
Takeuchi D, Saji T, Takatsuki S, Fujiwara M.	Abnormal Tissue Doppler Image are Associated with Elevated Plasma Brain Natriuretic Peptide and Increased Oxidative Stress in Acute Kawasaki Diseases.	Cric. J.	71	357-362	2007
Yoshidome Y, Morimoto S, Tamura N, Kobayashi S, Tsuda Hashimoto H, Takasaki Y.	A case of primary antiphospholipid antibody syndrome presenting with dysfunctional uterine bleeding and cerebral infarction.	Mod Rheumatol	17	251-2	2007
Tamura N, Matsudaira R, Hirashima M, Ikeda M, Tajima M, Nawata M, Morimoto S, Kaneda K, Kobayashi S, Hahimoto H, Takasaki Y.	Two cases of refractory Wegener's granylomatosis successfully treated with Ritsuximab.	Intern Med	46	409-14	2007
Matsumoto T, Kobayashi S, Ogishima D, Aoki Y, Sonoue H, Abe H, Fukumura Y, Nobukawa B, Kumasaka T, Mori S, Suda K.	Isolated necrotizing arteritis (localized polyarteritis nodosa): examination of the histological process and disease entity based on the histological classification of stage and histological differences from polyarteritis nodosa.	Cardiovasc Pathol	16	92-97	2007
Takahashi M, OtsuboS, Takei T, Sugiura H, Yoshida K, Tamei N, Koike M, Uchida K, Yumura W, Kawamura S, Horita S, Akiba T, Nitta K	Anti-glomerular basement membrane antibody disease with granulomatous lesions on renal biopsy.	Inten Med.	46(6)	295-301	2007
Yamazaki M, Takei T, Otsubo S, Iwasa S, Yabukui Y, Suzuki K, Koike M, Uchida K, Tsuchiya K, Yumura W, Horita S, Honda K, Akiba T, Nitta K	Wegener's granulomatosis complicated by intestinal ulcer due to cytomegalovirus infection and by thrombotic thrombocytopenic purpura.	Intern Med.	46(17)	1435-1440	2007

湯村和子	BVAS(Birmingham vasculitis activity score)とVDI(vasculitis damage index)	リウマチ科	37(3)	268-278	2007
此元隆雄、高橋真悠子、布井博幸	小児ネフローゼ症候群に対するミゾリビン一日一回投与の再発抑制効果	日本小児科学会雑誌	111	568-572	2007
Uezono S, Sato Y, Hara S, Hisanaga, S, Fukudome K, Fujimoto S, Nakao H, Kitamura K, Kobayashi S, Suzuki K, Hashimoto H, Nunoi H	Outcome of ANCA-associated primary renal vasculitis in Miyazaki Prefecture.	Intern Med	46	815-822	2007
藤元昭一	治癒可能な可逆性の腎不全-ANCA関連腎血管炎-	日州医事	No.689	97-98	2007
Ohno N	A murine model of vasculitis induced by fungal polysaccharide	Cardiovasc Hematol Agents Med Chem	6(1)	44-52	2008
Tada R, Nagi-Miura N, Adachi Y, Ohno N	The influence of culture conditions on vasculitis and anaphylactoid shock induced by fungal pathogen *Candida albicans* cell wall extract in mice	Microb Pathog	Epub 2007 Nov 9.		2007
Tada R, Nagi-Miura N, Adachi Y, Ohno N	An unambiguous assignment and structural analysis using solution NMR experiments of O-antigen from Escherichia coli ATCC23505 (Serotype O9)	Chem Pharm Bull	55(7)	992-995	2007
Tada R, Harada T, Nagi-Miura N, Adachi Y, Nakajima M, Yadomae T, Ohno N	NMR characterization of the structure of a beta-(1->3)-D-glucan isolate from cultured fruit bodies of Sparassis crispa	Carbohydr Res	342(17)	2611-2618	2007
Nagi-Miura N, Shingo Y, Kurihara K, Adachi Y, Suzuki K, Ohno N	Involvement of platelet activating factor, histamine and serotonin in acute lethal shock induced by Candida albicans water-soluble extracellular polysaccharide fraction (CAWS) in mice	Biol Pharm Bull	30(7)	1354-1357	2007
Ishida-Okawara A, Nagi-Miura N, Oharaseki T, Takahashi K, Okumura A, Tachikawa H, Kashiwamura S, Okamura H, Ohno N, Okada H, Ward PA, Suzuki K	Neutrophil activation and arteritis induced by C. albicans water-soluble mannoprotein-beta-glucan complex (CAWS)	Exp Mol Pathol	82(2)	220-226	2007

Okada N, Asai S, Hotta A, Miura N, Ohno N, Farkas I, Hau L, Okada H	Increased Inhibitory Capacity of an Anti-C5a Complementary Peptide Following Acetylation of N-terminal Alanine	Microbiol Immunol	51(4)	439-443	2007
高橋　啓	急性期動脈炎の病理組織像からみた川崎病の成因.	医学のあゆみ	222	855-858	2007
Takahashi K, Oharaseki T, Yokouchi Y, Naoe S, Jenette JC :	Kawasaki Disease Arterities and Polyarteritis Nodosa.	Pathology Case Reviews.	12	193-199	2007
大原関利章、高橋啓、横内　幸、直江史郎	川崎病の成因. 日本臨床 66:246-250, 2007	日本臨床	66	246-250	2007
Matthijsen, R.A., Huugen, D., Hoebers, N.T., Vries, B., Peutz-Kootstra, C. J., Aratani, Y., Daha, M.R., Tervaert, J. W. C., Buurman, W. A., and Heeringa, P	Myeloperoxidase is critically involved in the induction of organ damage following renal ischemia reperfusion.	Am. J. Pathol.	171	1743-1752	2007
Uno K, Hirosaki M, Kakimi K, Tominaga M, Suginoshita Y, Hasegawa G, Fukui M, Nakamura N, Shirakawa T, Kishida T.	Impaired IFN-alpha production and the risk of cancer development.	J Interferon Cytokine Res.	Dec;27 (12)	1013-7	2007
宇野賀津子、武曾恵理、尾松芳樹、八木克巳、猪原登志子、椛田美由紀、三石瑤子、村上善基、古宮俊幸、谷川真理、稲葉カヨ、鈴木和男、藤田哲也	健常人と各種疾患患者の末梢血のセンダイウイルス刺激IFN-α産生能とプラズマサイトイド樹状細胞数との相関	PASKEN JOURNAL	Vol.19 ,2006	1-6	2007
武曾恵理、鈴木進子、中川権史、辻井知美、古宮俊幸、米本智美、塚本達雄、魚瀬優、中村武志、猪原登志子、宇野賀津子、鈴木和男、岸田綱太郎	MPO-ANCA関連炎顕微鏡的多発血管炎に合併する悪性疾患症例の解析とIFN-α産生能からの考察	PASKEN JOURNAL	Vol.19 ,2006	7-11	2007
Ito-Ihara, T., Suzuki, K., Uno, K., Komiya, T., Tsujii, T., Tsukamoto, T., Ono, T., Fukatsu, A., Kita, T., Muso, E.	Circulating levels of IL-12, 23 and IL-18 in patients with MPO-ANCA-associated vasculitis.	Clinical Exp Rheumatology	vol.25, No.I, (Suppl.44)	S-89	2007
Muso, E., Uno, K., Ito-Ihara, T., Komiya, T., Suzuki, K.	Immunomodulatory effect of intravenous immunoglobulin (IVIg) therapy in MPO-ANCA related polyangitis with RPGN by amelioration of impaired IFNα production (IFN-P).	Clinical Exp Rheumatology	vol.25, No.I, (Suppl.44)	S-89	2007

Uno, K., Muso, E., Ihara, T., Komiya, T., Omatsu, Y., Mitsuishi, Y., Inaba, K., Suzuki, K.	Comparison of IFN-α production in response to Sendai virus upon stimulation and the number of peripheral plasmacytoid dendritic cells in healthy subjects and patients with various diseases: Characteristics of MPO-ANCA-associated glomerulonephritis and vasculitis.	Clinical Exp Rheumatology	vol.25, No.I, (Suppl.44)	S-90	2007
Uno K, Yagi K, Muso E, Omatsu Y, Ito-Ihara T, Mituishi Y, Murakami Y, Tanigawa M, Suzuki K, Fujita S	Comparison of HVJ stimulated IFN-a production & peripheral plasamacytoid dendritic cell counts in healthy subjects & patients with various diseases.	J IFN Cytokine Res.	Vol.27, No.8	734	2007
Tougan T, Onda H, Okuzaki D, Kobayashi S, Hashimoto H, Nojima H.	Focused microarray analysis of peripheral mononuclear blood cells from Churg-Strauss syndrome patients.	DNA Res.	15(1)	1-12.	2008
Yabuta, N., Okada, N., Ito, A., Hosomi, T., Nishihara, S., Sasayama, Y., Fujimori, A., Okuzaki, D., Zhao, H., Ikawa, M., Okabe, M. Nojima, H.	Lats2 is an essential mitotic regulator required for the coordination of cell division.	J. Biol. Chem.	282(26)	19259-19271	2007
Ohtaka, A., Okuzaki D, Saito,TT., Nojima H	Mcp4, a meiotic coiled-coil protein, plays a role in F-actin positioning during *Schizosaccharomyces pomb*	Eukaryot Cel	6(6)	971-983	2007

著書

著者氏名	論文タイトル名	書籍全体の編集者名	書籍名	出版社名	出版地	出版年	ページ
鈴木和男	好中球の機能調節	鈴木和男	生体防御医学事典	朝倉書店	東京	2007	164-169
湯村和子	ANCA関連腎炎の病態とモデルマウスでの知見	鈴木和男	生体防御医学事典	朝倉書店	東京	2007	304-308
平橋淳一	炎症における出血と血栓	鈴木和男	生体防御医学事典	朝倉書店	東京	2007	330-333

Microbiol. Immunol., 51(12), 1215–1220, 2007

Editor-Communicated Paper

Analysis of Risk Epitopes of Anti-Neutrophil Antibody MPO-ANCA in Vasculitis in Japanese Population

Kazuo Suzuki*[,1,†], Shigeto Kobayashi[2], Kazushige Yamazaki[3], Masaaki Gondo[3], Kazuo Tomizawa[1], Yoshihiro Arimura[4], Kimimasa Nakabayashi[4], Shoichi Ozaki[5], Masaharu Yoshida[6], Toshiharu Yoshida[7], Norimasa Tsusaka[8], Eri Muso[9], Tomio Okazaki[10], and Hiroshi Hashimoto[2]

[1]*Laboratory of Biodefense, Department of Bioactive Molecules, National Institute of Infectious Diseases, Shinjuku-ku, Tokyo 162–8640, Japan,* [2]*Department of Internal Medicine, Juntendo University School of Medicine, Bunkyo-ku, Tokyo 113–8421, Japan,* [3]*Teikoku Hormone Medical Co., Ltd., Minato-ku, Tokyo 107–0052 (Present address: ASAKA Pharmaceutical Co., Ltd., Minato-ku, Tokyo 108–8532), Japan,* [4]*The First Department of Internal Medicine, Kyorin University School of Medicine, Mitaka, Tokyo 181–8611, Japan,* [5]*Department of Internal Medicine, Graduate School of Medicine, Kyoto University, Kyoto, Kyoto 606–8501, Japan,* [6]*Department of Nephrology, Tokyo Medical University Hachioji Medical Center, Hachioji, Tokyo 193–0998, Japan,* [7]*Department of Internal Medicine, Fujita Health University, Toyoake, Aichi 470–1192, Japan,* [8]*Department of Internal Medicine, Saitama University Medical Center, Kawagoe, Saitama 350–8550, Japan,* [9]*Department of Internal Medicine, Graduate School of Medicine, Kyoto University, Kyoto, Kyoto 606–8501, Japan, and* [10]*Department of Pediatrics, Hiroshima City Hospital, Hiroshima, Hiroshima 730–8518, Japan*

Communicated by Dr. Toshinori Nakayama: Received October 9, 2007. Accepted October 16, 2007

***Abstract*: Autoantibodies to myeloperoxidase (MPO) are a subset of anti-neutrophil cytoplasmic antibody (ANCA, MPO-ANCA) detected in the sera of some patients with primary systemic vasculitis. The titer of MPO-ANCA does not always reflect disease activity and this inconsistency may be attributable to differences in epitopic specificity by MPO-ANCA among various patients with vasculitis. Epitope analysis may also explain the occurrence of MPO-ANCA in different vasculitic syndromes. We screened the sera of 148 MPO-ANCA positive patients from six vasculitic syndromes: rapidly progressive gromerulonephritis (RPGN), microscopic polyangiitis (MPA), idiopathic crescentic glomerulonephritis (I-CrGN), classic polyangiitis nodosa (cPAN), Churg-Strauss syndrome (CSS), Kawasaki disease (KD); and from patients with rheumatoid arthritis (RA) and systemic lupus erythematosus (SLE). The sera were collected by the Intractable Vasculitis Research Project Group in Japan. No serum showed epitopes La and Lb of light chain of MPO, and sera with 68.6% of patients showed a positive reaction to one or more epitopes in heavy chain of MPO. Analysis of binding level showed that RPGN, I-CrGN and MPA sera mainly reacted to the Ha epitope at the N-termimus of the MPO heavy chain, CSS sera reacted to Ha and the Hf epitope close to the C-terminus of the MPO heavy chain, KD reacted mainly to Hf, while SLE and RA sera reacted to all epitopes. These results suggest that MPO-ANCA recognizing specific regions of the N-terminus of the MPO H-chain confer an increased risk of vasculitis RPGN, I-CrGN, MPA and CSS. Furthermore, the epitopic specificity of MPO-ANCA differentiates vasculitic from non-vasculitic syndromes associated with MPO-ANCA positivity and differentiates in the cirtain type of vasculitis from various vasculitic syndromes. In particular, vasculitic syndromes associated with kidney involvement had similar epitopic reactivity which suggests that this pattern confers an increased risk of vasculitis.**

***Key words*: Myeloperoxidase (MPO), MPO-ANCA, Vasculitis, Epitope analysis, Rapidly progressive glomerulonephritis (RPGN), Microscopic polyangiitis (MPA), Kawasaki disease**

Autoantibies to myeloperoxidase (MPO-ANCA) are a subset of anti-neutrophil cytoplasmic antibodies (ANCA) and have been detected in the sera from patients with primary systemic vasculitis syndromes including microscopic polyangiitis (MPA) and rapidly progressive glomerulonephritis (RPGN). MPO-ANCA

has been demonstrated to be a good marker for the diagnosis of these disorders (1, 3, 5–7). The titer of MPO-ANCA is correlated with the activity of pauci-immune, necrotizing, crescentic glomerulonephritis. In addition, we have demonstrated a good correlation between the extent of crescent formation and the MPO-ANCA titer (1). However, a low titer of MPO-ANCA is found in the sera from some patients with active crescent formation, and conversely, high titer can be found during the remission stage. Therefore, it seems that the titer of MPO-ANCA is not always correlated with the activity of the disease due to difference in reactivity of MPO-ANCA to the MPO molecule. Such differences in reactivity suggests differences of binding to MPO epitopes by MPO-ANCA.

We have designed a panel of peptides to analyze the epitopes on MPO recognized by MPO-ANCA from patients with MPO-ANCA-associated vasculitis using recombinant MPO-fragments. A set of recombinant deletion mutants of MPO comprised eight fragments of the heavy-chain subunit, and two fragments of the light chain subunit, which were expressed in *E. coli*. The recombinant hexamer histidine-tagged fragments have been purified with a Ni^{2+}-charged nitrirotriacetic acid column. Reactivity of the recombinant fragments with a rabbit polyclonal antibody to human MPO has been assessed by immunoblotting and ELISA (4). Therefore, this panel was used in an ELISA system to subclassify MPO-ANCA-associated diseases (2, 8). Epitopes recognised by MPO-ANCA may also give clues to etiology and pathogenesis and may also be of prognostic value.

In the present study, we analyzed MPO epitopes using sera from patients with six vasculitic syndromes: rapidly progressive glomerulonephritis (RPGN), microscopic polyangiitis (MPA), idiopathic crescentic glomerulonephritis (I-CrGN), classic polyangiitis nodosa (cPAN), Churg-Strauss syndrome (CSS), Kawasaki disease (KD); and from patients with rheumatoid arthritis (RA) and systemic lupus erythematosus (SLE). The sera were collected from members and hospitals participating in a Japanese Inflactable Vasculitis project funded by the Ministry of Health and Welfare, Japan.

Materials and Methods

Chemicals. Ni^{2+}-charged nitrirotriacetic acid (Ni-NTA) resin was purchased from Qiagen GmbH (Hilden, Germany). Bacto-tryptone and bacto-yeast extract were obtained from Difco (Detroit, Mich., U.S.A.). Alkaline phosphatase (AP)-conjugated goat anti-rabbit IgG (H+L) (AP-ar-gIgG), nitroblue tetrazolium, 5-bromo-4-chloro-3 indolylphosphate in aqueous dimethylformamide and Tween-20, and 4-chloro-1-naphthol (4CN) were obtained from Japan Bio-Rad (Tokyo). Peroxidase-conjugated rabbit antihuman IgG specific for y chains (PO-ah-rIgG) and rabbit anti-human MPO were obtained from Dako A/S (Glostrup, Denmark). AP-conjugated goat anti-human IgG (H+L,

Table 1. Number of patients with vasculitis and number of serum with positive reactivity to each epitope site in various vasculitis examined

Syndrome	Total number of examined	No. of sera of patients with positive reactivity [a]						
		Ha	Hb	Hc	Hd	He	Hf	Hg
MPA	74	21	18	6	22	1	6	10
RPGN	8	3	2	2	2	0	0	1
I-CrGN	5	2	2	0	0	0	0	0
cPAN	3	3	0	0	1	1	1	0
CSS	3	1	1	1	0	0	1	0
KD	42	8	5	3	11	2	9	4
RA	9	4	0	0	4	0	0	2
SLE	4	3	3	1	2	2	2	3
Total	148	45	31	13	42	6	19	20

[a] Positive reactivity represented over the score 1. Some cases showed in two or more sites.

Address correspondence to Dr. Kazuo Suzuki, Department of Bioactive Molecules, National Institute of Infectious Diseases, Toyama, Shinjuku-ku, Tokyo 162–8640, Japan. Fax: +81–3–5285–1160, +81–43–221–0832 (present). E-mail: ksuzuki@nih.go.jp

†Present address: Inflammation Program, Department of Immunology, Chiba University Graduate School of Medicine, Chiba, Chiba 260–8670, Japan.

Abbreviations: ANCA, anti-neutrophil cytoplasmic antibody; cPAN, classic polyangiitis nodosa; CSS, Churg-Strauss syndrome; I-CrGN, idiopathic crescentic glomerulonephritis; KD, Kawasaki disease; MPA, microscopic polyangiitis; MPO, myeloperoxidase; RPGN, rapidly progressive glomerulonephritis; RA, rheumatoid arthritis; SLE, systemic lupus eryhtematosus.

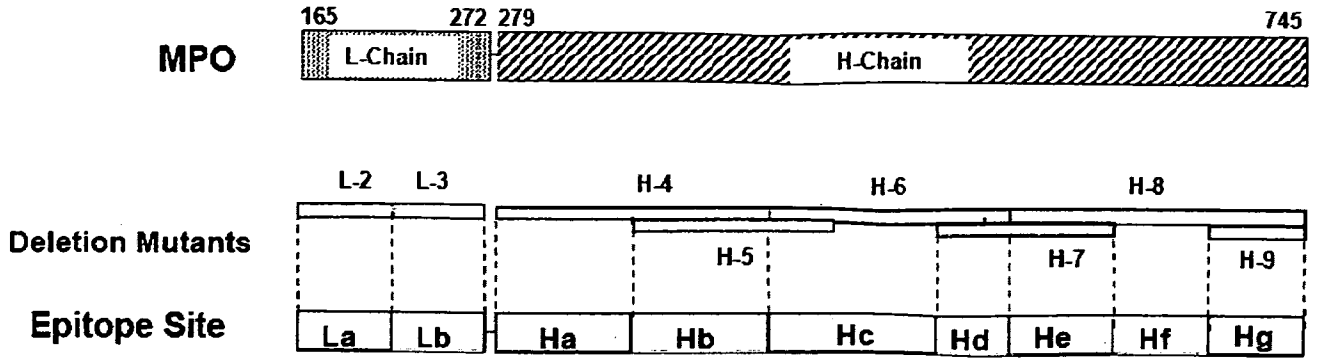

Fig. 1. Deletion mutants for epitope analysis of MPO-ANCA in serum of patients with vasculitis. Recombinant fragments of L-chain and H-chain of MPO were prepared using deletion mutants as described in "Materials and Methods."

AP-ah-gIgG) was obtained from ICN ImmunoBiologicals (San Francisco, Calif., U.S.A.). Lysozyme, *p*-nitrophenyl phosphate disodium and mineral oil were purchased from Sigma (St. Louis, Mo., U.S.A.). Block Ace was purchased from Yukijirushi Nyugyo Co., Ltd. (Sapporo, Japan).

Sera of patients with vasculitis. As shown in Table 1, sera of patients with RPGN, MPA, I-CrGN, cPAN, CSS, KD, RA and SLE in hospitals of Juntendo University, Kyorin University, Kyoto University, Tokyo Medical University, Fujita Health University, Saitama University Medical Center and Hiroshima City Hospital, were collected. All sera were collected following informed consent by the patients.

Preparation of recombinant fragment using deletion mutant of L-chain and H-chain of MPO. Eight fragments of MPO L-2, L-3, H-4, H-5, H-6, H-7, H-8 and H-9 were prepared as deletion mutants of MPO from *E. coli* described elsewhere (8). Briefly, recombinant L-2, L-3, H-4, H-5, H-6, H-7, H-8, and H-9 were expressed as shown in Fig. 1. Constructs in pQE32 Vectors *E. coli* cultured overnight in 300 to 1,200 ml of the medium was inoculated with 15 to 60 liters of Trific broth medium. Jar fermenters (B. E. Marubishi Co., Ltd., Tokyo) were set to keep dissolved oxygen above 40% by agitation at 400 rpm and aeration at 13 liters/min. The cells were further incubated at 37 C with shaking at 250 rpm. When the absorbance at 600 nm became approximately 0.7 to 0.9, IPTG (1 mM) was added, and the mixture incubated for a further 16 hr. The cells were harvested by centrifugation at 4,000 × *g* for 10 min and frozen at −80 C.

Purification of nine recombinant fragments. Insoluble proteins with a Ni-NTA column were denatured and purified. The frozen bacterial cells were thawed and suspended in Buffer A, consisting of 6 M guanidine-HCl, 0.1 M NaH_2PO_4, and 0.01 M Tris-HCl (pH 8.0), at a ratio of 5 ml/g wet weight. The cells were lysed by continuous mixing for 1 hr at room temperature. The cell debris was removed by centrifugation at 13,000 × *g* for 15 min. As the cell debris could not be removed completely when the jar fermenters were used, the cells were homogenized, sonicated, and filtrated through filter paper No. 5B (diameter, 95 mm) set on a Kiriyama Roto (Kiriyama Seisakusho, Ltd., Tokyo). The filtrate (2 to 40 ml) was applied to a Ni-NTA column (0.5 × 5, 2.5 × 10, or 2.5 × 20 cm) equilibrated with Buffer A. The column was washed with 20 column vol of Buffer A at a flow rate of 20 ml/hr and subsequently washed with 30 column vol of Buffer B, consisting of 8 M urea, 0.1 M NaH_2PO_4, and 0.01 M Tris-HCl (pH 8.0). The column was further washed with Buffer C, consisting of 8 M urea, 0.1 M NaH_2PO_4, and 0.01 M Tris-HCl (pH 6.3), until the A_{280} was below 0.1. The 6× His-tagged proteins were eluted with 50 ml of Buffer D, consisting of 8 M urea, 0.1 M NaH_2PO_4, and 0.01 M Tris-HCl (pH 5.9), followed by 20 to 100 ml of Buffer E, consisting of 8 M urea, 0.1 M NaH_2PO_4, and 0.01 M Tris-HCl (pH 4.5). Finally, any proteins remaining on the column were detached with Buffer F, consisting of 6 M guanidine-HCl and 0.2 M acetic acid (2, 8). The recombinant proteins fragments were completely purified. The eluate of the Ni-NTA column in Buffer D or E was applied to a Sephacryl S-200HR column (155 ml, 1.5 × 88 cm) equilibrated with 4 M urea containing 0.05 M sodium phosphate buffer (pH 7.2). All fragments except for H-2 were completely purified.

Determination of reactivity of serum for epitope estimation using nine recombinant fragments by ELISA. The protein solutions (1.7–6.8 μl) were added to a coating buffer containing 0.015 M sodium carbonate and 0.035 M sodium bicarbonate (pH 9.6) to make a concentration of 10 μg/ml of the protein. A 100-μl portion of the mixture was then plated to a well of a Nunc Immunoplate U96 Maxisorp (4-49824, Roskilde, Denmark) and kept overnight at room temperature. The plate was washed three times with a washing buffer consisting of 0.0025% Tween 20 and 0.15 mM sodium

azide in PBS(−). Blocking was carried out by Block Ace diluted with PBS(−) to 1/4. When the rabbit polyclonal anti-human MPO was used as a source of the first antibody, it was diluted to 1/500 with the dilution buffer. Every plate contained native MPO III (1 μg/well) as a positive control. The plate was incubated at room temperature for 1.5 hr. The plate was washed three times with washing buffer, and AP-ar-gIgG or AP-ah-gIgG diluted to 1/6,000 with the dilution buffer was added. The plate was washed three times with washing buffer. *p*-Nitrophenylphosphate as the AP substrate (100 xl) was added at a concentration of 1 mg/ml dissolved in substrate buffer consisting of 50 mM sodium carbonate buffer (pH 9.6) and 1 mM $MgCl_2$. After incubation for 60 min at room temperature, the plate was measured at double beam, 405 and 650 nm.

AP enzyme reaction was performed for 30 min at room temperature and measured at 405–650 nm by an ELISA reader (Bio-Rad). Epitope site was determined with a formula as follows.

% Prevalence of epitope site = (Pt_H-i/MPO-ANCA) − (Poly_H-i/MPO-ANCA) − (%Average H-i_NHS)

Formula:

Hence: Pt_H-i/MPO-ANCA = rate of reactivity of a serum of patient to H-i fragment/MPO-ANCA titer

Poly_H-i/MPO-ANCA = rate of reactivity of a polyclonal anti-MPO serum to H-i fragment/MPO-ANCA titer

%Average H-i_NHS = Average of reactivity of sera of 19 healthy controls to H-i fragment

Percent incidence of each epitope site in each serum was obtained ranging from 0 to 46% to make score ranging from 0 to 4: below 10%= score 0, 10–19%= score 1, 20–29%= score 2, 30–39%= score 3, 40–49%= score 4 and over 50%= score 5. Percent incidence of epitope in each disease was calculated by ratio of summation of score of serum among fragments in patients with each disease.

Absorbance of MPO-ANCA in sera of healthy volun-

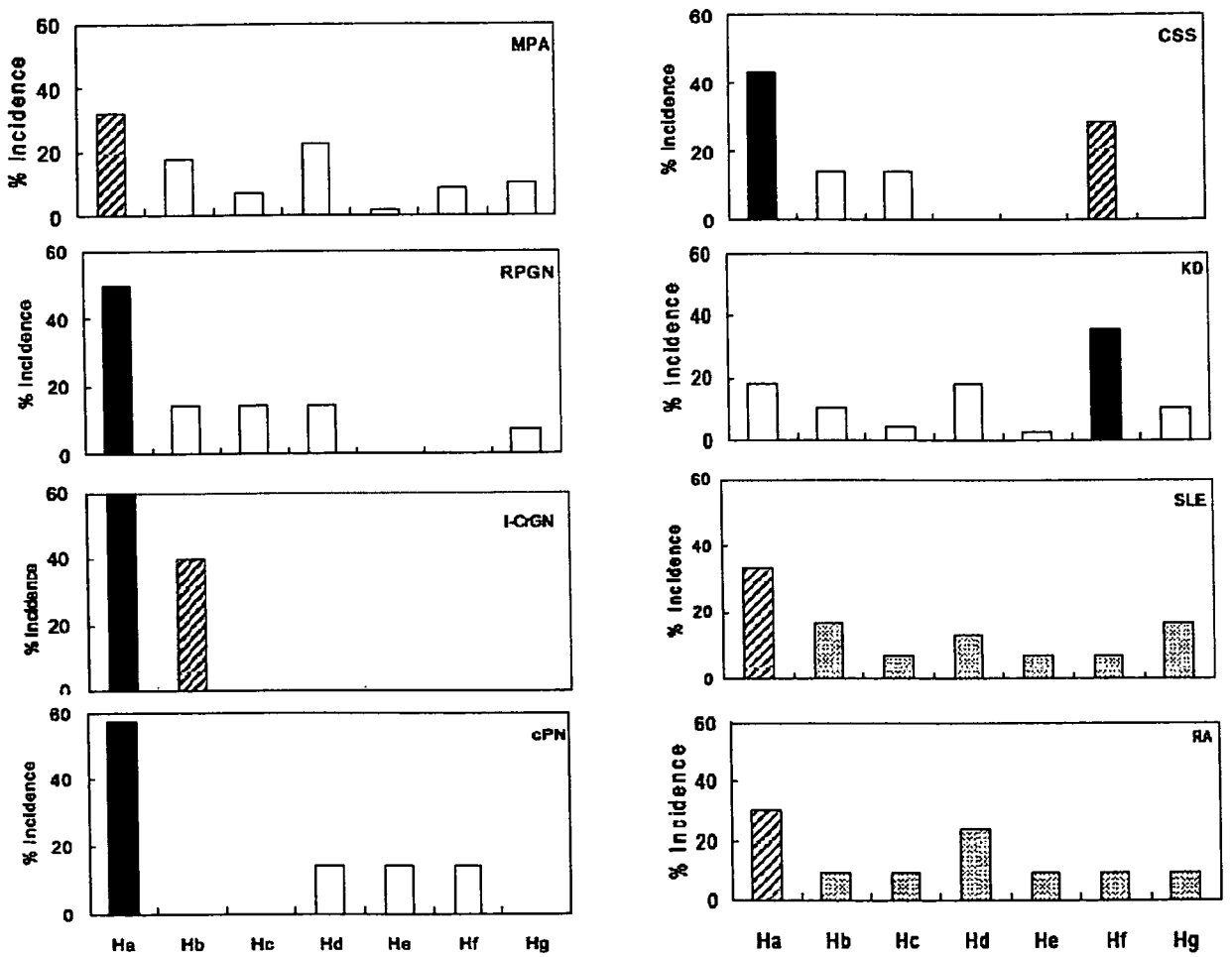

Fig. 2. Frequency of epitope sites of MPO-ANCA in serum of patients with vasculitis. Incidence in each vasculitis shows relative ratio (%) in all epitopes reacted with MPO fragments. Epitopes were calculated by a formula as described in "Materials and Methods."

teers (N = 19) was 0.272 ± 0.090 as Mean ± S.D.

Epitope sites were assigned as La, Lb, Ha, Hb, Hc, Hd, Hf and Hg by reactivity of sera to recombinant deletion mutants recombinant L-2, L-3, H-4, H-5, H-6, H-7, H-8, and H-9 (Fig. 1).

Results and Discussion

In primary systemic vasculitis, MPO-ANCA are a marker for diagnosis and have been implicated in pathogenesis of vasculitis. Although high MPO-ANCA titers are associated with increased risk of disease activity (1, 3, 5–7), MPO-ANCA titers do not necessarily correlate with disease activity or vasculitic syndrome. We have previously demonstrated that the severity of the diseases in CrGN is correlated with a particular epitopes of MPO-ANCA recognizing N- or C-terminus of the MPO heavy chain (2, 8).

In this study, we analyzed the epitope recognized by MPO-ANCA from sera of 148 patients with six vasculitic syndromes RPGN, MPA, I-CrGN, cPAN, CSS, KD, and from patients with RA and SLE in hospitals of members of the project funded by Ministry of Health, Lobour and Welfare. MPO-ANCA positive sera showed a positive reaction to one or more epitope sites of the MPO heavy chain in 68.6% of cases, but no epitopes in the MPO light chain. The sera reacted to each epitope site from Ha to Hg shown in Table 1. Furthermore, the binding level at each epitope site for the sera was estimated as scores of 1 to 5 and the incidence in each disease was calculated by a ratio of the summation of scores for each disease syndrome. According to the grading analysis, the percent incidences in each disease was shown in Fig. 2. As shown in Fig. 2, sera of RPGN confirmed the results of our previous study with reactivity to epitopes on the N-termimus of the MPO heavy chain. The ratio of reactivity of the sera on the N-terminus of the MPO heavy chain was 50% in all epitope sites examined. In addition, the ratio of the sera of patients with MPA also shows the highest prevalence with 32% in the N-terminus. In particular, sera of patients with I-CrGN was completely focused to the narrow epitopes on Ha and Hb. Moreover, sera of patients with cPAN reacted to the Ha region. However, the profile of sera from CSS was different with reactivity to the sites Ha in the N-terminus and Hf close to the C-terminus. Furthermore, the profile of sera of KD patients was quite different from these diseases with highest binding to Hf close to the C-terminus. Finally, sera of patients with RA and SLE reacted to all epitope sites. These results indicate that epitopes of MPO-ANCA were different among sera between vasculitic syndromes and non-vasculitis diseases. Moreover, the Ha region was recognized with sera from all diseases examined. In addition to ratio by scoring, 30.4% (45/148) of sera reacted to the Ha region when number of positive reaction of sera examined was determined.

The epitopic specificity of MPO-ANCA differentiates vasculitic from non-vasculitic syndromes associated with MPO-ANCA positivity and differentiates between vasculitic syndromes. In particular, vasculitic syndromes associated with kidney involvement had similar epitopic reactivity which suggests that this pattern confers an increased risk of vasculitis.

We thank colleagues in National Institute of Infectious Diseases, Japan, and Dr. David Jayne, Addenbrooke's Hospial, Cambridge, U.K. and Dr. Niels Rasmussen, the University of Copenhagen Health Sciences Hospital for valuable discussion. This study was supported in part by grants from Health Science Foundation and Ministry of Health and Welfare, Japan.

References

1) Arimura, Y., Minoshima, S., Kamiya, Y., Tanaka, U., Nakabayashi, K., Kitamoto, K., Nagasawa, T., Sasaki, T., and Suzuki, K. 1993. Serum myeloperoxidase and serum cytokines in anti-myeloperoxidase antibody-associated glomerulonephritis. Clin. Nephrol. **40**: 256–264.
2) Fujii, A., Tomizawa, K., Arimura, Y., Nagasawa, T., Y-Ohashi, Y., Hiyama, T., Mizuno, S., and Suzuki, K. 2000. Epitope analysis of myeloperoxidase-specific anti-neutrophil cytoplasmic antibody (MPO-ANCA) associated glomerulonephritis. Clin. Nephrol. **53**: 242–252.
3) Harper, J.M., Thiru, S., Lockwood, C.M., and Cooke, A. 1998. Myeloperoxidase autoantibodies distinguish vasculitis mediated by anti-neutrophil cytoplasm antibodies from immune complex disease in MRL/Mp-lpr/lpr mice: a spontaneous model for human microscopic angitis. Eur. J. Immunol. **28**: 2217–2226.
4) Ishida-Okawara, A., Ito-Ihara, T., Muso, E., Ono, T., Saiga, K., Nemoto, K., and Suzuki, K. 2004. Neutrophil contribution to the crescentic glomerulonephritis in SCG/Kj mice. Nephrol. Dial. Transplant. **19**: 1708–1715.
5) Neumann, I., Birck, R., Newman, M., Schnülle, P., Kriz, W., Nemoto, K., Yard, B., Waldherr, R., and Van Der Woude, F.J. 2003. SCG/Kinjoh mice: a model of ANCA-associated crescentic glomerulonephritis with immune deposits. Kidney Int. **64**: 140–148.
6) Savige, J., Gillis, D., Benson, E., Davies, D., Esnault, V., Falk, R.J., Hagen, E.C., Jayne, D., Jennette, J.C., Paspaliaris, B., Pollock, W., Pusey, C., Savage, C.O., Silvestrini, R., van der Woude, F., Wieslander, J., and Wiik, A. 1999. International consensus statement on testing and reporting of antineutrophil cytoplasmic antibodies (ANCA). Am. J. Clin. Pathol. **111**: 507–513.
7) Savige, J., Dimech, W., Fritzler, M., Goeken, J., Hagen, E.C., Jennette, J.C., McEvoy, R., Pusey, C., Pollock, W., Trevisin, M., Wiik, A., and Wong, R. 2003. Addendum to the international consensus statement on testing and reporting of antineutrophil cytoplasmic antibodies. Quality control

guidelines, comments, and recommendations for testing in other autoimmune diseases. Am. J. Clin. Pathol. **120**: 312–318.

8) Tomizawa, K., Mine, E., Fujii, A., Y-Ohashi, Y., Yamagoe, S., Ishida-Okawara, A., Hashimoto, Y., Ito, M., Tanokura, M., Yamamoto, T., Arimura, Y., Nagasawa, T., Mizuno, S., and Suzuki, K. 1998. A panel set for epitope analysis of myeloperoxidase (MPO)-specific anti-neutrophil cytoplasmic antibody MPO-ANCA using recombinant hexamer histidine-tagged MPO deletion mutants. J. Clin. Immunol. **18**: 142–152.

THE JOURNAL OF BIOLOGICAL CHEMISTRY VOL. 282, NO. 38, pp. 27994–28003, September 21, 2007
Printed in the U.S.A.

Impact of Two Novel Mutations on the Structure and Function of Human Myeloperoxidase*

Received for publication, March 7, 2007, and in revised form, July 23, 2007 Published, JBC Papers in Press, July 24, 2007, DOI 10.1074/jbc.M701984200

Melissa Goedken[‡], Sally McCormick[‡], Kevin G. Leidal[‡], Kazuo Suzuki[§], Yosuke Kameoka[¶], Joshua M. Astern[‖], Meilan Huang[**], Artem Cherkasov[**], and William M. Nauseef[‡1]

*From the [‡]Inflammation Program, Department of Medicine, University of Iowa and Veterans Affairs Medical Center, Iowa City, Iowa 52241, [§]National Institute of Infectious Diseases, Toyama 1-23-1, Shinjuku-ku, Tokyo 162 8640, Japan, [¶]Laboratory of Genetic Resources, Division of Biomedical Resources, National Institute of Biomedical Innovation, 7-6-8, Saitoasagi, Ibaraki-City, Osaka, 567-0085, Japan, [‖]University of North Carolina, Kidney Center, Chapel Hill, North Carolina 27599, and **Division of Infectious Diseases, Department of Medicine, Faculty of Medicine, University of British Columbia, Vancouver V5Z 3J5, British Columbia, Canada*

The heme protein myeloperoxidase (MPO) contributes critically to O_2-dependent neutrophil antimicrobial activity. Two Japanese adults were identified with inherited MPO deficiency because of mutations at Arg-499 or Gly-501, conserved residues near the proximal histidine in the heme pocket. Because of the proximity of these residues to a critical histidine in the heme pocket, we examined the biosynthesis, function, and spectral properties of the peroxidase stably expressed in human embryonic kidney cells. Biosynthesis of normal MPO by human embryonic kidney cells faithfully mirrored events previously identified in cells expressing endogenous MPO. Mutant apopro-MPO was 90 kDa and interacted normally with the molecular chaperones ERp57, calreticulin, and calnexin in the endoplasmic reticulum. However, mutant precursors were not proteolytically processed into subunits of MPO, although secretion of the unprocessed precursors occurred normally. Although δ-[^{14}C]aminolevulinic acid incorporation demonstrated formation of pro-MPO in both mutants, neither protein was enzymatically active. The Soret band for each mutant was shifted from the normal 430 to ~412 nm, confirming that heme was incorporated but suggesting that the number of covalent bonds or other structural aspects of the heme pocket were disrupted by the mutations. These studies demonstrate that despite heme incorporation, mutations in the heme environs compromised the oxidizing potential of MPO.

Phagocytes contribute significantly to human innate immunity, and polymorphonuclear neutrophils (PMN)[2] are the predominant granulocyte in the circulation. When PMN are deficient in number or function, normal antimicrobial action is severely compromised, resulting in increased morbidity and mortality from infection. Well suited for the wide diversity of potential microbial challenges, PMN possess a broad array of responses by which to contain, control, kill, and degrade microorganisms, both in the phagosome and within the immediate cellular environs. These defenses include degradative and antimicrobial proteins, fabricated during myeloid development and stored within the granules, as well as reactive oxygen and nitrogen species generated *de novo* specifically in response to invasion. None of these elements functions alone, but rather there is extensive and overlapping collaborations within the context of the phagosome.

The most extensively studied example of the synergistic antimicrobial systems within human PMN is the myeloperoxidase-H_2O_2-halide system (1). PMN simultaneously activate the normally dormant NADPH oxidase and release granule contents in response to stimulation. The H_2O_2 produced by the multicomponent phagocyte NADPH oxidase (2) converts the azurophilic granule protein myeloperoxidase (MPO) from its resting state into compound I, a transient intermediate with potent oxidizing properties, which in turn oxidizes Cl^- to Cl^+, thereby generating the potent antimicrobial agent HOCl (3). In addition to HOCl, chloramines and other longer lived products of the MPO-H_2O_2-halide system have been implicated in mediating cytotoxicity to a broad array of microorganisms as well as mammalian proteins and cells (4–10). In its capacity as a peroxidase, the activity of MPO depends on a normal heme group, which in the case of MPO is a ferric protoporphyrin IX covalently linked to the protein backbone (11, 12). Data from the crystal structure of native human MPO indicate that the heme group stably interacts with the protein backbone via three covalent bonds and eight hydrogen bonds (11). Structural features unique to the heme group of MPO make it the only member of the animal peroxidase family capable of oxidizing chloride and thus generating HOCl, at physiologic pH (13–15).

Significant insights into the normal biosynthesis, structure, and function of MPO have been derived from studies of the functional impact of inherited mutations (reviewed in Ref. 6 and see Refs. 16–20). To date, none of the previously characterized genotypes has directly involved the region around the

* This work was supported by National Institutes of Health Grant HL 53592 and a Merit Review from Veterans Affairs (to W. M. N.). The costs of publication of this article were defrayed in part by the payment of page charges. This article must therefore be hereby marked "*advertisement*" in accordance with 18 U.S.C. Section 1734 solely to indicate this fact.

[1] To whom correspondence should be addressed: Inflammation Program, and Dept. of Medicine, Roy J. and Lucille A. Carver College of Medicine, University of Iowa, D160 MTF, 2501 Crosspark Road, Coralville, IA 52241. Tel.: 319-335-4278; Fax: 319-335-4194; E-mail: william-nauseef@uiowa.edu.

[2] The abbreviations used are: PMN, polymorphonuclear neutrophil; MPO, myeloperoxidase; HEK, human embryonic kidney; PIPES, 1,4-piperazinediethanesulfonic acid; EPO, eosinophil peroxidase; LPO, lactoperoxidase; TPO, thyroid peroxidase; ER, endoplasmic reticulum; CRT, calreticulin; CLN, calnexin.

heme group of MPO. However, missense mutations at residue 501[3] (glycine to serine, G501S) and residue 499 (arginine to cysteine, R499C) have been identified in two unrelated Japanese individuals with inherited MPO deficiency (21, 22). We describe here the structural and functional consequences caused by G501S and R499C, two mutations adjacent to the critical histidine 502 on the proximal side of the heme in MPO.

EXPERIMENTAL PROCEDURES

Materials—K562 erythroleukemia cells and human embryonal kidney 293 (HEK) cells were obtained from American Type Culture Collection (Manassas, VA), ATCC CCL 243 and CRL-1573, respectively. Vectors pREP10 and pcDNA3.1 and antibiotics hygromycin and G-418 sulfate were obtained from Invitrogen; [^{35}S]methionine/cysteine (26.7×10^7 Bq/0.5 ml) was from Amersham Biosciences. δ-[^{14}C]Aminolevulinic acid (45.7 mCi/mmol) was custom-made by PerkinElmer Life Sciences. All tissue culture reagents were obtained from the University of Iowa Hybridoma Facility. Antibodies against calnexin and ERp57 were obtained from StressGen Bioreagents (Ann Arbor, MI). The monospecific rabbit antibody against human myeloperoxidase was generated in our laboratory (23), as was the rabbit antibody against human calreticulin (24), the latter available commercially from Affinity Bioreagents (Golden, CO). Endoglycosidase H and *N*-glycosidase F from *Chryseobacterium meningosepticum* were obtained from Calbiochem. Unless otherwise specified, all other reagents were purchased from Sigma.

Molecular Modeling—Reasoning that the missense mutations at residues 499 and 501 might adversely influence the structure around the heme in MPO, we modeled the active site of native and mutant forms of the protein. To that end, the three-dimensional structure of human MPO protein was retrieved from the protein data base (Protein Data Bank code 1D2V), and its heme-containing domain was subjected to simplistic energy minimization. For all three structures, we performed force field-based energy minimization of side chains in proximity to the heme to gain insight into the geometry and possible conformational changes of critical residues at the atomic level. We considered the heme, iron, and bromide ions and close proximity residues (Fig. 1). Mutant MPO structures were derived from the native MPO crystal structure by the *in silico* replacement of Arg-499 with cysteine and Gly-501 with serine using a molecular modeling package (Molecular Operation Environment, version 2004.10, Chemical Computation Group). The geometry of introduced residues of the mutant forms in the active site was minimized using the CHARMM 22 force field (25). The hydrogen atoms were added to the structures of native and mutated MPO protein using CHARMM HBUILD module, and their positions were further optimized.

Stably Transfected Cells Lines—K562 erythroleukemia cells were maintained in RPMI 1640 medium with 10% fetal calf serum, 2 mM L-glutamine, and penicillin/streptomycin at 37 °C in an atmosphere of 5% CO_2 (18). HEK cells were maintained in Dulbecco's modified Eagle's medium/Ham's nutrient mixture F-12 medium supplemented with 10% fetal calf serum, 100 units/ml penicillin, 100 μg/ml streptomycin, 100 mM HEPES, and 2 mM L-glutamine. Stably transfected cell lines expressing G501S and R499C were created using the same approaches previously employed to analyze normal and specific mutants of human MPO (17). PCR was used to mutate Gly-501 or Arg-499 in normal MPO cDNA for heterologous expression in human cell lines that are devoid of endogenous MPO. The forward and reverse primers for mutagenesis of Gly-501 were GCCTTCCGCTACAGCCACACCCTCA and TGAGGGTGTGGCTGTAGCGGAAGGC, respectively, with the mutated residue indicated in boldface type, whereas primers ACCAATGCCTTCTGCTACGGCCACA and TGTGGCCGTAGCAGAAGGCATTGTT were used to create R499C. The presence of the desired mutation and absence of unintentional mutations were confirmed by sequencing the cDNA prior to transfection. Once the sequence of the desired mutant construct was confirmed, it was cloned into the expression vector (pREP10 for K562 cells and pcDNA3.1(−) for HEK cells). Stable transfectants were cloned by limiting dilution and selected using hygromycin and G-418 sulfate, respectively.

MPO Biosynthesis by Transfectants—Stable transfectants were used for the expression of wild-type and mutant forms of MPO (17, 18, 24, 26). Cells were maintained at low density in media supplemented with 2 μg/ml hemin for 24 h prior to labeling and placed in methionine-free RPMI medium supplemented with fetal calf serum and antibiotics for 1 h prior to pulse labeling with [^{35}S]methionine/cysteine. Cells were labeled for the indicated period and then recovered or chased by the addition of 1000-fold excess of cold methionine, before solubilization for subsequent analysis.

MPO-related products were immunoprecipitated using antibodies against MPO, CRT, or CLN. Biosynthetically radiolabeled MPO-related proteins in cell lysates or culture medium were immunoprecipitated with monospecific, polyclonal rabbit anti-human MPO (17, 18, 24, 26–31) separated by SDS-PAGE, followed by autoradiography, and quantitated by direct measurement of radioactivity using a PhosphorImager (Typhoon 9410, Amersham Biosciences).

MPO-related species that were associated with CRT or CLN were recovered and quantitated using sequential immunoprecipitations (17, 24, 26). Cell lysates were immunoprecipitated first with CRT or CLN antiserum under nondenaturing conditions. The CRT- or CLN-associated proteins in the recovered complex were released by heating in the presence of 2% SDS, and the solution was cooled and diluted 10-fold before proceeding with the immunoprecipitation with MPO antiserum. CRT- and CLN-associated MPO species were separated by SDS-PAGE and quantitated using the PhosphorImager.

Heme acquisition was assessed by radiolabeling with δ-[^{14}C]aminolevulinic acid, a precursor in heme synthesis, as done previously. Stable transfectants expressing normal or mutant MPO were cultured in the presence of δ-[^{14}C]aminolevulinic acid overnight, followed by solubilization and immunoprecipitation of the cell lysate or conditioned culture media with MPO antibody, as described above. MPO species containing ^{14}C were quantitated with the PhosphorImager.

[3] Because considerations of MPO include the propeptide, our amino acid designations are 166 greater (for the 166 amino acids in the propeptide) than those used by Fenna and co-workers (11, 53).

MPO Activity—Four different assays were employed to assess MPO activity. Peroxidase activity of the expressed wild-type or mutant MPO was quantitated in two complementary ways. Nontransfected cells, normal MPO transfectants, and transfectants expressing mutant MPO were cultured in the presence of 2 μg/ml hemin for 48 h prior to recovery and solubilization for determination of enzymatic activity. Peroxidase activity was quantitated spectrophotometrically using *o*-dianisidine as a substrate (32). Peroxidase activity in cell lysates was also assessed by *in situ* staining in a native polyacrylamide gel. Duplicate samples were electrophoresed under nondenaturing conditions into two 10% polyacrylamide gels containing 0.05% (w/v) cetyltrimethylammonium bromide and 25% glycerol (w/v) in the absence of a stacking gel. Samples were electrophoresed at constant voltage (100 V) toward the cathode until the dye front was ~5 mm from the bottom of the gel (~5 h). To avoid permanently staining the Scotch Brite pads with crystal violet, we often electrophorese the dye front off the gel (800–1000 V-h) when subsequently blotting native gels. One gel was washed and stained with trimethylbenzidine to assess peroxidase activity (33–35). The other gel was soaked in transfer buffer for 1 h and then subjected to electroblotting to a nitrocellulose filter for 850 V-h. The resulting blot was blocked and then processed with MPO antiserum. By performing both analyses in parallel, peroxidase activity could be assigned to a specific protein immunochemically related to MPO.

The greater amounts of mutant protein generated by HEK transfectants made possible two additional assays that are specific for MPO. We quantitated the capacity of HEK cell lysates, either wild-type or transfectants expressing normal or mutant MPO, to consume H_2O_2, using a H_2O_2 electrode and modification of a method described previously (36). In the presence of chloride, H_2O_2 consumption by MPO reflected HOCl production. The electrode (Apollo 4000, World Precision Instruments, Sarasota, FL) was calibrated daily with dilutions of reagent grade H_2O_2 (0–20 mM), with the concentrations of the H_2O_2 standard verified spectrophotometrically using $\epsilon_{240} = 43.6\ M^{-1}\ cm^{-1}$ (37). Cell lysates were added to known amounts of H_2O_2 in the presence of taurine, to scavenge HOCl and thus eliminate the possibility of its inactivation of the MPO (36), and the rate of H_2O_2 consumption was measured polarigraphically. Data are expressed as nanomoles H_2O_2 consumed per min per cell eq.

The lysates were likewise assessed for MPO-specific chlorinating capacity using the taurine chloramine assay (36). HOCl reacts with taurine to generate taurine monochloramine, which in turns reacts with 5-thio-2-nitrobenzoic acid to generate 5,5′-dithiobis(2-nitrobenzoic acid). The concentration of taurine monochloramine measured spectrophotometrically, $\epsilon_{412} = 14.1\ M^{-1}\ cm^{-1}$, and its loss were monitored as a reflection of HOCl production. Lysates from wild-type or transfected cells were used as the potential peroxidase source, and acetaldehyde-xanthine oxidase served as a source for generating oxidants. Data are expressed as nanomoles of HOCl produced/min. All assays were performed in triplicate, and each experiment was performed at least three times. We confirmed our findings in a more sensitive and specific assay for MPO-dependent chloramine production that uses iodide-dependent oxidation of 3,3′,5,5′-tetramethylbenzidine as substrate (38). As little as 200 pM MPO can be detected using this assay.

Glycosidase Susceptibility of MPO-related Proteins—Modifications of the carbohydrate side chains on MPO-related proteins were assessed by their relative susceptibility to endoglycosidases as done previously with MPO endogenously expressed in myeloid precursors (31, 39). MPO-related proteins were immunoprecipitated from cell lysates or culture medium at specified time points and treated with endoglycosidase H or *N*-glycanase to digest high mannose or complex carbohydrate side chains, respectively. Digested proteins and control immunoprecipitates were separated by SDS-PAGE and visualized by autoradiography.

Spectroscopy—Just as the endogenous MPO synthesized by myeloid precursors is largely compartmentalized into an intracellular organelle (1), MPO expressed by HEK cells was stored in membrane-bound organelles that could be recovered by differential centrifugation. HEK cells ($1–2.5 \times 10^8$) were collected, treated with diisopropylfluorophosphate, washed, and resuspended in relaxation buffer (10 mM PIPES, 100 mM KCl, 3 mM NaCl, 3.5 mM $MgCl_2$, 1 mM ATP, pH 7.3) at 2×10^7/ml. Cells were then disrupted by N_2 cavitation (350 p.s.i.), and the cavitate was collected in a volume of EGTA, pH 7.4, to achieve a final concentration of 1.25 mM, using a method employed previously for recovering intact intracellular organelles from human neutrophils (40) and cultured promyelocytic cell lines (32). Unbroken cells and nuclei were removed by low speed centrifugation, and the supernatant was centrifuged at $12,000 \times g$ for 20 min (4 °C) to recover a pellet enriched for dense intracellular organelles, including those containing MPO-related proteins. The pellet was resuspended in phosphate-buffered saline without calcium or magnesium, washed, and lysed by three freeze-thaw cycles using vigorous pipetting. Vigorous pipetting at each step was essential to maximize vesicle disruption. The clarified supernatant after pellet lysis was scanned from 400 to 600 nm in a Lambda 40 spectrophotometer (PerkinElmer Life Sciences). In addition, oxidation-reduction difference spectroscopy was performed, using dithionite to reduce the lysate in the sample cuvette. The concentration of normal MPO was calculated for oxidized samples using $\epsilon_{430} = 91\ mM^{-1}\ cm^{-1}$ (41). For turbid samples reduced minus oxidized difference spectra were obtained, and the concentration was calculated using $\epsilon_{473} = 75\ mM^{-1}\ cm^{-1}$ (41). For assays using mutant MPO, the same extinction coefficients were employed to approximate the concentrations of G501S and R499C.

RESULTS

Identification of MPO-deficient Subjects—As part of ongoing studies of the prevalence of inherited MPO deficiency in Japan (42), individuals with partial or complete deficiency were identified using automated flow hematocytochemistry to screen large populations. Among these deficient individuals were two with missense mutations in MPO, G501S, and R499C, that had not been reported previously. In both cases, the individuals were asymptomatic and had not suffered from frequent or severe infectious complications, as described in the detailed clinical reports (21, 22, 42).

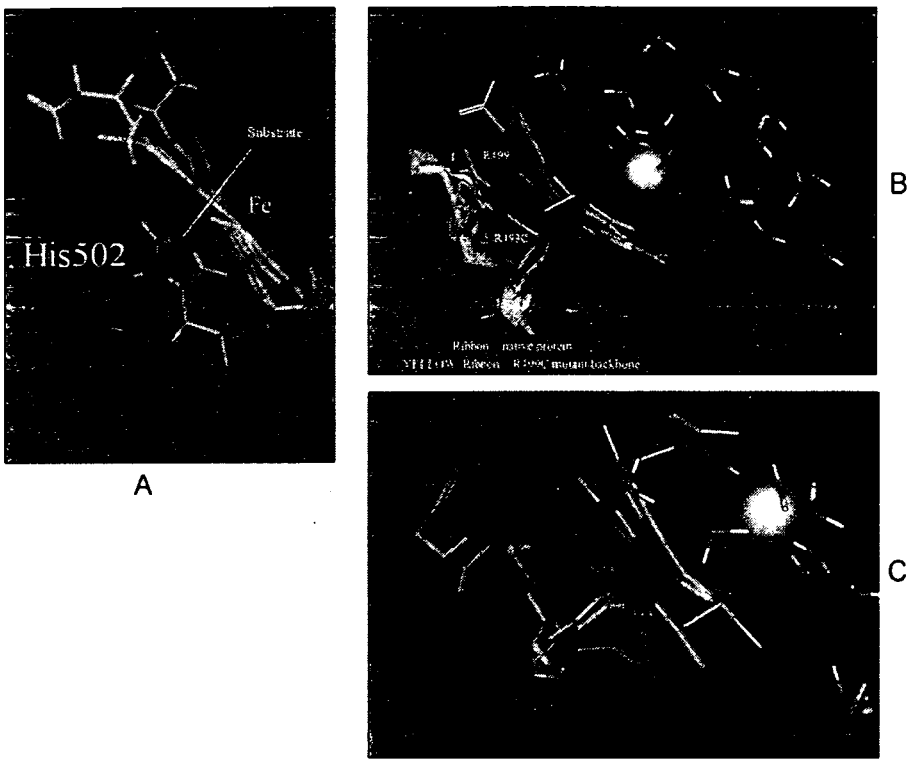

FIGURE 1. **Models of the heme pockets of normal and mutant MPO.** *A*, proximal heme-binding residue, His-502, and heme iron are depicted in a CPK model. His-502 anchors 6-coordinated Fe^{3+} ion of the heme from the underneath position, leaving the sixth coordination site above the heme available to react with substrate. *B*, normal MPO is depicted in *green*, R499C in *yellow*, and bromide (representing the halide-binding site) in *orange*. The proximity of the sulfur atom of the cysteine of R499C is sufficient to exert significant electrostatic effect on the heme iron. *C*, normal MPO is depicted in *green*, with G501S in *gray*. Because of steric limitations, the replacement of glycine with serine at residue 501 may significantly compromise heme binding. Furthermore, if possible, substitution of the flexible Gly-501 residue with serine would compromise backbone flexibility (backbone "hinge") in the heme pocket and consequently promote the departure of the His-502 anchoring side chain from the iron ion.

Predictions Derived from Molecular Modeling—Given the availability of the crystal structure of human MPO (11), we modeled the heme pocket of specific mutants at residues 499 and 501 for comparison with the native protein and to gain insight into their potential impact on MPO enzymatic activity. The iron ion in native MPO has six coordination sites as follows: four sites are mediated by pyrrole nitrogen atoms in the heme, and the fifth coordination is the axial His-502–iron bond. The sixth coordination site on the iron ion is vacant and serves to accept electrons and thereby participate in the electrochemistry of the iron-catalyzed oxidation (43) (Fig. 1*A*).

The heme in MPO is covalently bound to the protein through two ester linkages and a methionyl sulfonium linkage (11). In addition to the three covalent bonds, electrostatic interactions with pyrrole rings C and D contribute to the structure and stability of the heme pocket in MPO. The guanidinium group of Arg-499, as well as that of Arg-590, forms hydrogen bonds with the carboxyl group of a propionate in ring D (11). Replacement of Arg-499 with any residue that eliminates this electrostatic interaction would likely compromise heme binding and stability. Furthermore, after arranging the side chains in R499C to optimize favorable interactions with the molecular neighbors, the model of the heme pocket predicted sufficient space and side chain mobility to afford close proximity between its sulfur atom and the heme iron, if heme were incorporated into the pocket lacking the stabilizing arginine at 499. Whether in a neutral or deprotonated state, the sulfur introduced by R499C could coordinate with the iron, thereby forming a relatively strong interaction at ~2.5 Å (Fig. 1*B*). Such strong polar or covalent interaction could significantly compromise redox properties of the iron ion and thereby compromise the enzymatic activity of the mutant protein. Thus, the model predicts two consequences from R499C, one reflecting the loss of an important stabilizing electrostatic interaction with arginine and the other the introduction of a disruptive cysteine.

The optimized model of G501S likewise demonstrated potential changes that could compromise the function of the heme (Fig. 1*C*). The replacement of glycine with serine may leave inadequate space to stably accommodate the heme group. Furthermore, if the substitution was tolerated, replacement of glycine with serine would reduce the flexibility of the protein backbone in the heme environs. Although the highly flexible Gly-501 in native MPO allows close approximation of the aromatic nitrogen in His-502 below the heme iron atom, the loss of flexibility after the serine replacement might disturb proper heme function. Taken together, the simplistic models of each of the naturally occurring mutations in such close proximity to the redox center of MPO predicted structural consequences likely to compromise optimal function of the heme group.

Failure of G501S Precursor to Undergo Proteolytic Maturation—To examine directly the impact of these missense mutations on the fate of the protein, we created stable transfectants and compared synthesis of the mutant proteins with that of normal MPO. Stably transfected K562 cells expressing normal or G501S MPO were radiolabeled for 1 h and chased for 0 or 20 h before recovery of cells and the conditioned medium for immunoprecipitation. K562 transfectants expressing either normal or G501S MPO synthesized a 90-kDa protein after 1 h of labeling (Fig. 2). In the case of normal MPO, the 90-kDa protein underwent proteolytic processing during the 20 h of chase to yield the 59- and 13.5-kDa subunits of mature MPO. However, the precursor in G501S cells failed to yield the 59-kDa heavy subunit, and more of the 90-kDa precursor was present during the chase period in G501S-expressing cells than in transfectants expressing normal MPO, indicating that the absence of mature MPO reflected failure to undergo processing into MPO subunits and not the rapid degradation of the mutant G501S precursor.

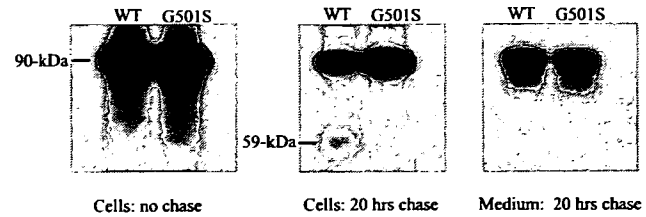

FIGURE 2. **Biosynthesis of normal and G501S MPO by transfected K562 cells.** K562 cells stably transfected with wild-type MPO (*WT*) or G501S mutant MPO (G501S) were pulse-labeled with [^{35}S]methionine and chased for 0 or 20 h. Cell lysates at 0 and 20 h and culture medium at 20 h were immunoprecipitated with anti-MPO. Immunoprecipitates were separated by SDS-PAGE, and dried gels were subjected to autoradiography. Cells expressing G501S synthesized and secreted a 90-kDa precursor form of MPO but failed to process it into the mature MPO, represented by the generation of the 59-kDa heavy subunit of the native protein.

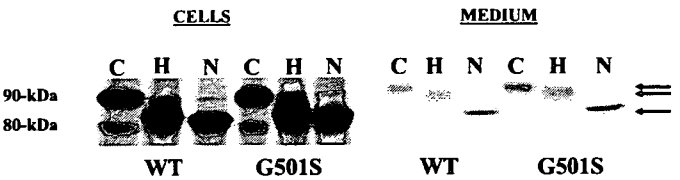

FIGURE 3. **Glycosylation of normal and G501S MPO produced by K562 transfectants.** After 1 h of biosynthetic pulse labeling with [^{35}S]methionine and a 20-h chase, cell lysates and culture medium from K562 cells expressing normal (*WT*) or mutant (G501S) MPO were immunoprecipitated with anti-MPO. Immunoprecipitates were incubated with buffer alone (*C*), endoglycosidase H (*H*), or *N*-glycanase (*N*) before recovery and analysis by SDS-PAGE and autoradiography. Fully glycosylated precursor migrated at 90 kDa, whereas the nonglycosylated product was 80 kDa. *Arrows* indicate individual glycosylated products. For both normal and mutant MPO, secreted MPO precursors were more resistant to endoglycosidase H digestion than were the intracellular forms.

Normal and G501S-expressing cells secreted the same amounts of 90-kDa MPO protein into the culture medium during the chase period (Fig. 2), suggesting that normal amounts of the G501S precursor entered the secretory pathway despite the failure of proteolytic maturation to proceed. As reported previously for normal MPO biosynthesis (20), ~10% of MPO precursor is secreted constitutively and undergoes limited modification of its oligosaccharide side chains during transit through the Golgi, whereby the secreted species is partially resistant to endoglycosidase H digestion (39). To determine whether the secreted MPO precursor from transfectants expressing G501S underwent oligosaccharide modification, the lysates of pulse-labeled cells and supernatants conditioned by the 20-h chase period were recovered from each cell line, immunoprecipitated with MPO antiserum, and subjected to digestion with endoglycosidase H or *N*-glycanase to cleave high mannose or both high mannose and complex mannose side chains, respectively. The oligosaccharides on the intracellular 90-kDa MPO precursors of normal and G501S were both fully susceptible to digestion with endoglycosidase H, indicating that the side chains were exclusively high mannose in nature (Fig. 3). However, the carbohydrates on the secreted MPO precursor were partially endoglycosidase H-resistant, as evidenced by limited digestion with endoglycosidase H but complete removal by *N*-glycanase treatment. The G501S mutant behaved in a fashion identical to that of normal MPO, suggesting that the G501S precursor entered the constitutive secretory pathway and was modified by Golgi resident enzymes in a normal fashion.

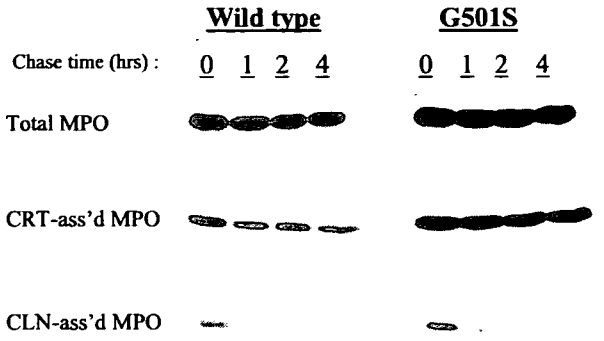

FIGURE 4. **Association of molecular chaperones with normal and G501S MPO in K562 cells.** K562 transfectants expressing normal (*wild type*) or G501S MPO were biosynthetically radiolabeled for 1 h and chased with cold methionine for 0–4 h. Cell lysates were immunoprecipitated with anti-MPO or sequentially with anti-CRT or anti-CLN followed by anti-MPO. Resulting immunoprecipitates were analyzed by SDS-PAGE and autoradiography. Like normal MPO, the G501S precursor associated transiently with CRT and CLN.

During normal biosynthesis MPO precursors interact transiently with calreticulin (CRT), calnexin (CLN), and ERp57 (20), all molecular chaperones in the ER that contribute to the proper folding of many glycoproteins (44). Pulse-labeled K562 cells transfected with normal or G501S MPO were chased for 0, 1, 2, or 4 h, and the lysates were immunoprecipitated in parallel with antibodies against MPO, CRT, or CLN under nondenaturing conditions, as described previously. To recover the CRT- and CLN-associated MPO precursor at each time point, the immunoprecipitates were denatured and subjected to a second immunoprecipitation using the MPO antibody (Fig. 4). In both transfectants expressing normal and G501S MPO, the recoveries of CRT-associated and CLN-associated MPO precursor were the same as reported previously for normal MPO (24, 26), suggesting that the interactions between CRT or CLN with MPO precursors were not significantly altered by the G501S missense mutation.

Activity of G501S Precursors Expressed in K562 Cells—Normal MPO biosynthesis requires the insertion of heme into apopro-MPO in the ER, thereby converting an enzymatically inactive 90-kDa MPO precursor into a 90-kDa protein with peroxidase activity (45). We assessed first the peroxidase activity of the G501S product spectroscopically using *o*-dianisidine as the substrate. K562 cells lack endogenous MPO (18) and exhibited very low background peroxidase activity in this assay (0.9 IU). In contrast, an identical number of PLB-985 cells, a human promyelocytic cell line that actively synthesizes structurally and functionally normal MPO (24), had 17.2 IU of peroxidase activity. K562 cells transfected with normal MPO had 4.9 IU of peroxidase activity (n = 5), whereas G501S transfectants had 0.5 IU of activity, levels indistinguishable from base line. Because we were concerned that the relatively low efficiency of MPO expression in the K562 cell system might undermine our capacity to detect very low levels of activity by the G501S, we examined the suitability of using HEK cells for biosynthetic studies, based on its successful application to generating recombinant protein for use in immunological characterization of anti-MPO-mediated vasculitis (46).

MPO Biosynthesis by HEK Transfectants—Wild-type HEK cells lack endogenous MPO, but after transfection synthesized

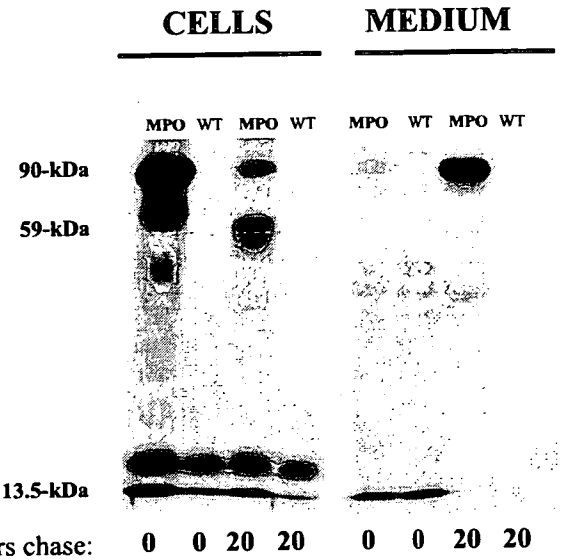

FIGURE 5. **Biosynthesis of normal MPO by stably transfected HEK cells.** Wild-type HEK cells (*WT*) or HEK cells stably expressing normal MPO were biosynthetically radiolabeled, with intervals of chase of 0 and 20 h. Cell lysates and culture medium were immunoprecipitated with anti-MPO and the immunoprecipitates analyzed by SDS-PAGE and autoradiography. Wild-type HEK cells lacked endogenous MPO. When expressed in HEK cells, MPO precursors were synthesized, secreted, and proteolytically processed intracellularly in a fashion identical to that seen in myeloid cells expressing endogenous MPO.

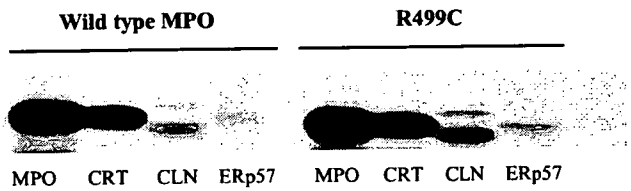

	MPO	R499C
CRT-associated	34.2%	33.6%
CLN-associated	4.6%	3.7%
ERp57-associated	1.9%	2.9%

FIGURE 6. **Association of molecular chaperones with normal MPO in stably transfected HEK cells.** Stably transfected HEK cells expressing normal (wild-type MPO) or R499C mutant were biosynthetically radiolabeled for 1 h and immunoprecipitated with anti-MPO or antibodies against the molecular chaperones CRT, CLN, or ERp57 under nondenaturing conditions. Immunoprecipitates were analyzed by SDS-PAGE and autoradiography. Molecular chaperones coprecipitated with precursors of normal and mutant MPO (results representative of three independent experiments).

heme-containing precursors that underwent normal proteolytic processing to mature MPO and efficient targeting to an intracellular, membrane-bound compartment that could be pelleted by centrifugation (Fig. 5). All aspects of MPO biosynthesis seen in cultured myeloid cells were reproduced in the HEK-MPO system. Specifically, the 90-kDa apopro-MPO acquired heme in the ER to form pro-MPO and precursors interacted with molecular chaperones ERp57, CRT, and CLN (Fig. 6) with the same selectivity previously reported for the K562 transfectants (24, 26). Heme acquisition was necessary for exit from the ER and for proteolytic processing to mature subunits, with the latter event inhibited by disruption of the Golgi by treatment with brefeldin A (data not shown). Approximately 10% of MPO precursor entered the secretory pathway and underwent limited modification of its oligosaccharide side chains, as seen with MPO endogenously produced by cultured promyelocytes (39). The spectral properties of MPO-enriched pellets recovered from stable transfectants were identical to those of normal MPO (see below), with a λ_{max} of 430 nm for the oxidized sample and a Soret band at 473 nm for the reduced minus oxidized spectroscopy (41). Taken together, the data indicate that the HEK transfectants faithfully mirrored the events in normal MPO biosynthesis previously identified in myeloid precursors.

Most important for our studies was the improved level of MPO expression in HEK cells relative to that in the K562 transfectants. Wild-type HEK cells lack any evidence of endogenous MPO, as judged immunochemically, spectroscopically, or by assessing enzymatic activity. In contrast, the specific activity of HEK-MPO (4.2 nmol of H_2O_2 consumed per min/pmol MPO, $n = 3$) was the same as partially purified MPO recovered from granules of normal PMN (3.3 nmol of H_2O_2 consumed per min/pmol MPO, $n = 3$) or the human promyelocytic cell line PLB-985 cultured in hemin (3.6 nmol of H_2O_2 consumed per min/pmol MPO, $n = 3$). Although the amount of MPO in transfectants (3.9 pmol of MPO/10^6 cells, $n = 3$) was lower than that in normal PMN (11.7 pmol of MPO/10^6 cells, $n = 3$) or in PLB-985 cells grown in the presence of hemin (11 pmol of MPO/10^6 cells, $n = 3$), HEK transfectants provided a system to yield levels of protein sufficient to perform spectroscopy and reliably assess function of specific mutants.

HEK-R499C, a Second Mutation Near the Critical Proximal Histidine in the Heme Pocket—To assess the impact of the R499C missense mutation on MPO biosynthesis both in relation to normal MPO and to G501S, we created stably transfected HEK cell lines expressing the mutant forms of MPO. After 1 h of biosynthetic labeling with [^{35}S]methionine, HEK-R499C associated with CRT, CLN, and ERp57 to the same extent as did wild-type MPO (Fig. 6), and the rates of dissociation during the chase were likewise the same (data not shown). Both R499C and G501S lacked enzymatic activity in native activity gels (Fig. 7). The HEK-R499C resembled G501S with respect to proteolytic processing, as both mutations resulted in synthesis of a 90-kDa species that was secreted normally but was not processed into mature subunits after a 20-h chase (Fig. 8*A*). As both mutants were enzymatically inactive and failed to undergo normal maturation, we anticipated that neither incorporated heme. However, transfectants expressing normal or mutant MPO and labeled with δ-[^{14}C]aminolevulinic acid, a precursor of heme, synthesized the 90-kDa pro-MPO that was released into the culture medium (Fig. 8*B*). When normalized for the [^{35}S]methionine content in MPO precursors, heme incorporation was 28.7 ± 2.9 and 23.7 ± 1.6% of control for R499C and G501S, respectively ($n = 3$). Based on these data and the amount of heme in HEK-MPO cells (3.9 pmol/10^6 cells), we estimate that R499C and G501S transfectants contained ~1.12 and 0.92 pmol of heme-containing MPO-related protein per 10^6 cells. Thus, in both mutants there was a maturation arrest at the stage of heme incorporation, whereby heme acquisition by mutant apopro-MPO was inefficient or the mutant pro-MPO was unstable and rapidly degraded. The stability of the mutant precursors was not increased by culturing cells in the presence of proteasome inhibitors (data not shown), in contrast to the

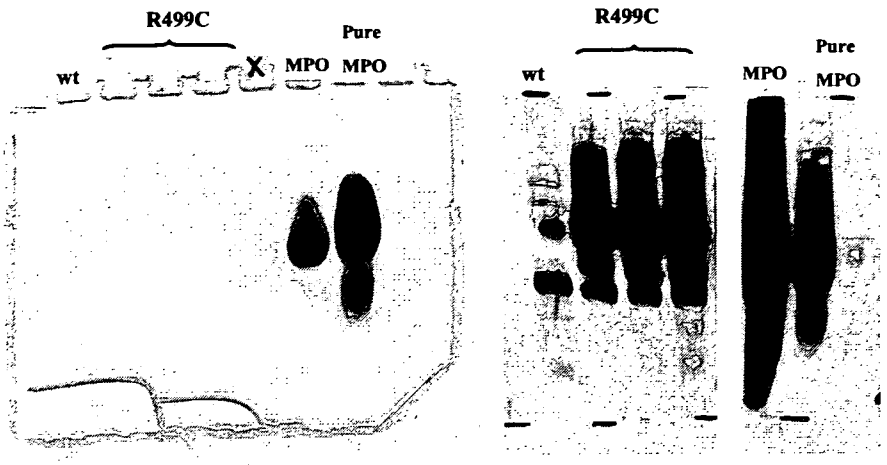

A) Native activity gel B) Immunoblot of native gel

FIGURE 7. **Peroxidase activity of R499C MPO.** Wild-type HEK cells, HEK cells stably transfected with R499C or normal MPO (MPO), or purified MPO (2 μg) were separated in two identical native gels. Resultant gels were stained for peroxidase activity (*A*) or electroblotted to nitrocellulose and probed with anti-MPO (*B*). No peroxidase activity was identified in HEK cells or in R499C-HEK cells, whereas HEK-MPO cells exhibited peroxidase activity (*A*). The lack of activity in R499C-HEK cells did not reflect the absence of the mutant protein from the gel, as demonstrated by the presence of immunoreactive protein in the R499C-HEK cell immunoblot (*B*).

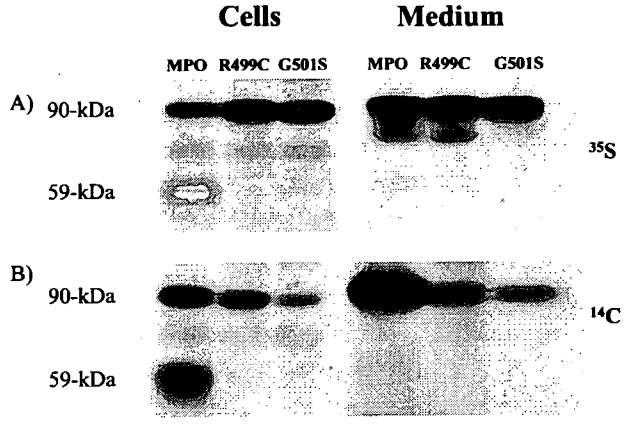

FIGURE 8. **Biosynthetic incorporation of heme into normal, R499C, and G501S MPO.** HEK transfectants expressing normal MPO, R499C, or G501S were pulse-labeled with [^{35}S]methionine and chased for 20 h (*A*) or labeled with δ-[^{14}C]aminolevulinic acid (*B*). The resultant cell lysates and culture media were immunoprecipitated with anti-MPO and analyzed by SDS-PAGE and autoradiography. Given the relative specific activities of the radioisotopes used, autoradiographs were exposed for 6 h or 11 days for ^{35}S and ^{14}C, respectively. Although heme was incorporated into the 90-kDa pro-MPO and 59-kDa mature subunit in HEK-MPO cells, heme acquisition for G501S and R499C was limited to the mutant 90-kDa pro-MPO form. When normalized for the amount of [^{35}S]methionine-labeled MPO precursor, heme incorporation for G501S and R499C was 23.7 ± 1.6 and 28.7 ± 2.9% of that for normal MPO. Values represent mean ± S.E., $n = 3$.

proteasome-mediated degradation seen with the MPO mutant Y173C (17), indicating that if degradation of mutant proteins occurred, it was not mediated by the proteasome.

Given the failure of either mutant to exhibit peroxidase activity *in vitro*, we anticipated that neither would chlorinate taurine. Neither G501S nor R499C chlorinated taurine (data not shown), and the capacity for G501S or R499C to consume H_2O_2 was low, 0.52 and 0.65 nmol/min/cell eq, respectively, and no different from that of wild-type HEK cells (0.91 nmol/min/cell eq). In contrast, HEK transfectants expressing normal MPO were fully active (5.75 nmol/min/cell eq), suggesting that although the mutant had incorporated heme, the resultant pro-MPO was not competent to mediate peroxidative events. To compare the spectral properties of normal and mutant proteins, samples enriched for the intracellular compartment in HEK cells containing normal and mutant MPO were prepared. The presence of MPO-related proteins in each pellet was confirmed by immunoblotting (data not shown). Although all four samples had identical spectra in the 200–400 nm range (data not shown), significant differences were noted in the Soret absorbance region. Wild-type HEK cells lacked a Soret peak between 400 and 500 nm (Fig. 9), whereas the pellets recovered from normal PMN or from HEK transfectants expressing normal MPO exhibited a peak at 430 nm, characteristic of MPO (41). In contrast, pellets from HEK transfectants expressing R499C or G501S exhibited a Soret band at 414 nm, with no detectable signal at 430 nm. The observed red shift of the absorbance peak in the mutant proteins suggests that each of the alterations near histidine 502, critical for binding on the proximal side of the heme, altered the structural conformation of the heme.

DISCUSSION

Mature MPO normally resides exclusively in the azurophilic granules of PMN and monocytes, compartments containing a variety of hydrolytic enzymes (for review of MPO biology see Ref. 1). Concomitant activation of the NADPH-dependent oxidase, a source of reactive oxygen species including H_2O_2, and release of granule contents, including MPO, into the newly formed phagolysosome, deliver to the ingested microorganism a variety of toxic reactants that synergistically mediate efficient killing (reviewed in Ref. 3). Among these noxious agents is HOCl, the result of the unique property of MPO to catalyze the 2-electron peroxidation of Cl^- in the presence of H_2O_2 (47). HOCl is extremely toxic to bacteria; 10^8 HOCl molecules/cell can kill 5 g of *Escherichia coli*, whereas $>10^{11}$ molecules of H_2O_2 (under metal-free conditions) or hydroxyl radical are necessary to achieve the same cytotoxicity (48–50). Several lines of evidence support the importance of the MPO-H_2O_2-Cl^- system in oxygen-dependent microbicidal activity against a wide spectrum of organisms, including viruses, bacteria, fungi, protozoa, and tumor cells as well as promoting inflammation *per se* (reviewed in Ref. 47). Given that MPO and its unique chemistry appear especially well suited for a central role in antimicrobial activity, elucidation of critical structural determinants is essential to understand the basis for its biological action.

Heme peroxidases can be categorized into three superfamilies based on sequence: catalases, plant peroxidases, and mammalian peroxidases (51). Mammalian peroxidases include the cyclooxygenase and myeloperoxidase families, the latter com-

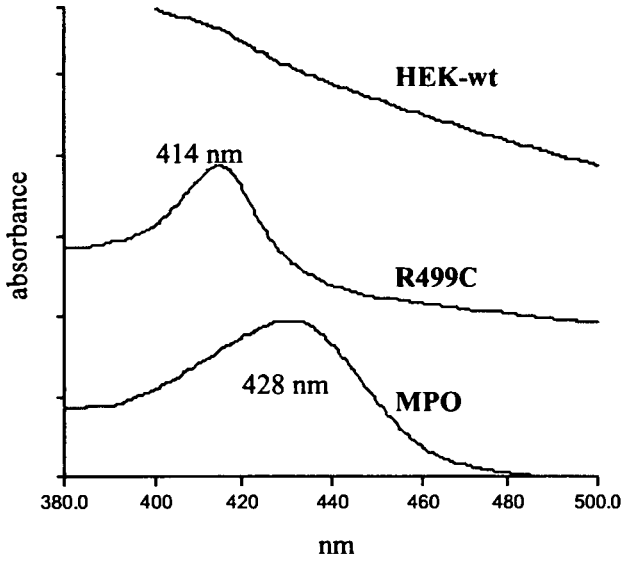

FIGURE 9. **Spectral properties of normal and R499C MPO.** The 48,000 × *g* pellet recovered from wild-type (*WT*) HEK cells or from HEK cells stably expressing normal MPO or the R499C mutant was scanned spectrophotometrically. Whereas pellets from wild-type HEK lysates lacked a Soret band, cells expressing normal MPO exhibited the ~430 nm peak characteristic of MPO. In contrast, the peak from R499C-HEK cells was shifted to 414 nm. Spectra are representative of three independent experiments.

posed of MPO, eosinophil peroxidase (EPO), lactoperoxidase (LPO), and thyroid peroxidase (TPO) (52, 53). These peroxidases share the unique property of having two or three covalent bonds between the heme and the mature enzyme. Availability of an expression system for MPO biosynthesis and processing that faithfully mirrors the endogenous events in myeloid cells is an analytical tool necessary for the study of structure-function relationships in the heme pocket of animal peroxidases. Previous studies of the structural features of the heme environment of MPO that employed mutagenesis (reviewed in Ref. 54) relied on recombinant protein isolated from transfectants unable to synthesize the functional, normal subunits of MPO. The recombinant MPO produced in Chinese hamster ovary cells used for these studies has oligosaccharide side chains significantly different from native MPO, fails to undergo proteolytic processing into mature subunits, and is expressed only in the monomeric form (55). Such differences may have functional consequences. For example, mutation of Met-409 to the corresponding residue in EPO (Thr), TPO (Val), or LPO (Gln) altered the spectral properties of the recombinant protein and eliminated its peroxidase activity (56), an unexpected finding given that this replacement normally exists in these related peroxidases. Given the quality control operative in the ER during MPO biosynthesis (17, 57, 58), it is possible that the observed deviations from normal biosynthesis have structural consequences that may undermine the interpretation of studies using the Chinese hamster ovary-derived recombinant protein.

Although K562 transfectants expressing normal MPO recapitulate biosynthetic events seen in myeloid cells expressing endogenous MPO, the yields of recombinant protein are insufficient for structural or functional studies. As an essential component of this study, we established that HEK cells stably transfected with normal MPO exhibited seminal features of the biosynthesis and proteolytic processing of MPO as first characterized in myeloid precursors (reviewed in Ref. 17 and see Refs. 18, 24, 26, 28, 30, 31, 57, 59–63). The primary translation product in HEK cells underwent cotranslational cleavage of the signal peptide, *N*-linked glycosylation, and limited deglucosylation of high mannose oligosaccharide side chains to generate the 90-kDa, enzymatically inactive precursor apopro-MPO that interacted in the ER transiently and reversibly with the molecular chaperones ERp57, CRT, and CLN with subsequent incorporation of heme to generate the enzymatically active 90-kDa pro-MPO. Heme synthesis inhibition blocked proteolytic maturation as well as export of MPO precursor from the ER, indicating that its acquisition of heme induced conformational changes necessary for successful maturation and intracellular targeting. Although 10% of pro-MPO entered the secretory pathway and was recovered from the culture media, as reported for myeloid cells (64, 65), most pro-MPO underwent modification of oligosaccharide side chains and proteolytic processing *en route* to a membrane-bound intracellular compartment. We believe that our expression system provides sufficient material that mirrors the native protein and is thus especially well suited to address several specific questions of structure-function relationships raised by its crystal structure.

Among the animal peroxidases, only MPO has been crystallized, with structures of both the human and canine enzyme published. Based on the crystal structure of human MPO at 1.8 Å (11), the heme pocket is in a crevice ~15–20 Å deep and is solvent-accessible via an open channel at the catalytic site on the distal side of the heme (53). There is significant amino acid identity among the animal peroxidases in the four helices that surround the heme group, and several lines of evidence (4, 66–68) implicate five residues in binding heme in MPO. Histidines at residues 261 and at 502 represent the distal and proximal ligands, respectively, and heme is covalently bound to MPO at three sites as follows: through a methionyl sulfonium linkage with Met-409 and through ester linkages to Glu-408 and Asp-260 (11, 69). The heme-protein interaction is further stabilized by hydrogen bonding between the carbonyl groups of ring C and D propionates and Thr-266, Asp-264, Arg-499, Arg-590, and water molecules (11). Although crystal structures for other family members have not been solved, modeling of homologous domains, NMR, mass spectrometry, and peptide analysis support the presence of the same two ester linkages in LPO, EPO, and TPO (11, 70–74). Ester bonds account for the 10 nm shift in the Soret band of LPO, EPO, and TPO relative to horseradish peroxidase, and the presence of the third covalent bond in MPO causes the red shift of the Soret band of oxidized MPO (λ_{max} = 430 nm) relative to the spectral peak for the other family members (λ_{max} = 412 nm) (73, 75, 76). The peculiar sulfonium linkage in MPO likely contributes as well to its unique facility to oxidize Cl^- to HOCl at physiologic pH. The presence of covalent bonds between the prosthetic group and the protein is a feature unique to the animal peroxidases (51), and a H_2O_2-dependent autocatalytic process has been implicated in ester bond formation (72), although the precise mechanisms of ester bond formation in animal peroxidases and of sulfonium linkage in MPO *in vivo* are unknown. Although at least one covalent bond is required for peroxidase activity and the presence of covalent bonds with heme is a feature shared by